

# Lines of interacting quantum-dot cells: A binary wire

Craig S. Lent and P. Douglas Tougaw

Department of Electrical Engineering, University of Notre Dame, Notre Dame, Indiana 46556

(Received 23 February 1993; accepted for publication 2 August 1993)

The behavior of linear arrays of cells composed of quantum dots is examined. Each cell holds two electrons and interacts Coulombically with neighboring cells. The electrons in the cell tend to align along one of two axes resulting in a cell "polarization" which can be used to encode binary information. The ground-state polarization of a cell is a highly nonlinear function of the polarization of its neighbors. The resulting bistable saturation can be used to transmit binary information along the line of cells, thus forming a binary wire.

## I. INTRODUCTION

Many investigators have noted the connection between quantum devices and locally interconnected architectures.<sup>1</sup> The small currents and charges inherent in quantum devices are poorly suited for driving large numbers of devices, particularly conventional devices. Requiring that a quantum device interact only with its neighbors is much more promising. Despite the appeal of this synthesis, few proposals including both a specification of the component quantum devices and the coupling between them have appeared.<sup>2</sup>

Recently, a specific proposal for a quantum cellular automata (QCA) implementation has been made by the authors *et al.*<sup>3,4</sup> The scheme is based on a quantum cell composed of several quantum dots and containing two electrons. Coulomb repulsion between the electrons causes the charge in the cell to align along one of two directions. These two alignment states, "polarizations," are used to encode binary information. The Coulomb coupling of the charge distribution in one cell to the charge in neighboring cells provides a physics-based local coupling between cells. The coupling leads to a highly bistable saturation behavior in the polarization, avoiding some of the criticisms of usual quantum interference-based device characteristics.<sup>5</sup> Specific arrangements of cells which can function as AND and OR gates have been proposed.

In this article we examine in detail the linear arrays of such quantum-dot cells which form the "wires" in the QCA scheme proposed. In the following section we review the physics of the basic cell and the model proposed in Ref. 3. Section III presents the theoretical machinery, a Hartree self-consistency scheme, which we use to examine arrays of cells. Section IV contains the examination of the behavior of a linear array of cells. We show that for a large range of physical parameters, the linear array behaves as a binary wire. Section V contains a discussion of the results.

## II. COUPLED QUANTUM CELLS

The quantum-dot cell is shown schematically in Fig. 1(a). It consists of four quantum dots on the corners of a square and one central dot.<sup>6</sup> The cell is occupied by two electrons.<sup>7,8</sup> Tunneling occurs between near neighbors and next-nearest neighbors but the barriers between cells are assumed sufficient to completely suppress electron tunnel-

ing between cells. We treat the quantum dots in the site representation, ignoring any degrees of freedom within the dot.

### A. Cell polarization

The Coulomb interaction causes the two electrons to tend to occupy antipodal sites. The two-electron ground state may then consist of the electrons aligned along one of two perpendicular axes as shown in Fig. 1(b). We define a quantity called the cell polarization which measures the extent to which the charge is aligned along one of these two axes. We denote the single-particle density at site  $i$  as  $\rho_i$ . The polarization is then defined as

$$P \equiv \frac{(\rho_1 + \rho_3) - (\rho_2 + \rho_4)}{\rho_0 + \rho_1 + \rho_2 + \rho_3 + \rho_4}. \quad (1)$$

If the two electrons are entirely localized in sites 1 and 3, then the polarization  $P=1$ . If the electrons are on sites 2 and 4,  $P=-1$ . An isolated cell would have a ground state which is a linear combination of these two polarizations, hence a net polarization of zero.<sup>9</sup>

### B. The cell Hamiltonian

We construct a simple model of the cell using a tight-binding Hubbard-type Hamiltonian. For an isolated cell, the Hamiltonian can be written

$$H_0^{\text{cell}} = \sum_{i,\sigma} E_0 n_{i,\sigma} + \sum_{i>j,\sigma} t_{i,j} (a_{i,\sigma}^\dagger a_{j,\sigma} + a_{j,\sigma}^\dagger a_{i,\sigma}) + \sum_i E_Q n_{i,\uparrow} n_{i,\downarrow} + \sum_{i>j,\sigma,\sigma'} V_Q \frac{n_{i,\sigma} n_{j,\sigma'}}{|\mathbf{R}_i - \mathbf{R}_j|}. \quad (2)$$

Here  $a_{i,\sigma}$  is the annihilation operator which destroys a particle at site  $i$  ( $i=0,1,2,3,4$ ) with spin  $\sigma$ . The number operator for site  $i$  and spin  $\sigma$  is represented by  $n_{i,\sigma}$ . The on-site energy for each dot is  $E_0$ , the coupling between the  $i$ th and  $j$ th dot is  $t_{i,j}$ , and the on-site charging energy (the Coulomb cost for two electrons of opposite spin occupying the same dot) is  $E_Q$ . The last term in the Hamiltonian represents the Coulombic potential energy for two electrons located at sites  $i$  and  $j$  at positions  $\mathbf{R}_i$  and  $\mathbf{R}_j$ .

For our "standard cell," on which most of the numerical results reported here are based, we obtain the values of the parameters in the Hamiltonian from a simple, experi-

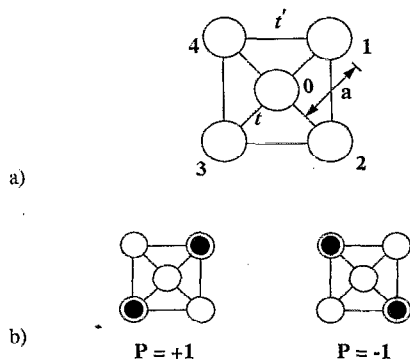


FIG. 1. Schematic of quantum cell. The geometry of the cell is shown in (a). The solid lines indicate tunneling between the quantum dots. The tunneling energy between the inner dot and the outer dots is  $t$ , and the tunneling energy between adjacent outer dots is  $t'$ . The Coulomb repulsion between the two electrons which occupy the cell results in ground-state configurations with the electrons aligned in the two orientations shown in (b). The polarization defined by Eq. (1) takes the values 1 and  $-1$  for these two configurations.

mentally reasonable model. We take  $E_0$  to be the ground-state energy of a circular quantum dot with diameter  $D=10$  nm holding an electron with effective mass  $m^*=0.067m_0$ . The near-neighbor distance between dot centers  $a$  is taken to be 20 nm. The Coulomb coupling strength  $V_Q$  is calculated for a material with a dielectric constant of 10. We take  $E_Q=V_Q/(D/3)$ . The coupling energy between the outer dots and the central dot is  $t \equiv t_{0,i}=0.3$  meV ( $i=1,4$ ), and the next-nearest neighbor coupling connecting the outer dots,  $t'$ , is taken to be  $t/10$  (consistent with one-dimensional calculations for reasonable barriers). The range of possible values of these parameters is explored systematically below where we show that the important bistable saturation behavior is present for a wide range of parameters.

The interaction of the cell with the surrounding environment, including other neighboring cells, is contained in a second term in the Hamiltonian which we write as  $H_{\text{inter}}^{\text{cell}}$ . We solve the time-independent Schrödinger equation for the state of the cell  $|\Psi_n\rangle$  under the influence of the neighboring cells;

$$(H_0^{\text{cell}} + H_{\text{inter}}^{\text{cell}}) |\Psi_n\rangle = E_n |\Psi_n\rangle. \quad (3)$$

The spins of the two electrons in a cell can be either aligned or antialigned, with corresponding changes in the spatial part of the wave function due to the Pauli principle. We will restrict our attention to the case of antialigned spins here because that is the ground-state configuration; the spin-aligned case exhibits nearly identical behavior. The Hamiltonian is diagonalized directly in the basis of few-electron states. We calculate single particle densities  $\rho_i$  from the two-particle ground-state wave function  $|\Psi_0\rangle$ ,

$$\rho_i = \sum_{\sigma} \langle \Psi_0 | n_{i,\sigma} | \Psi_0 \rangle, \quad (4)$$

and from the densities, calculate the resultant polarization  $P$  from Eq. (1).

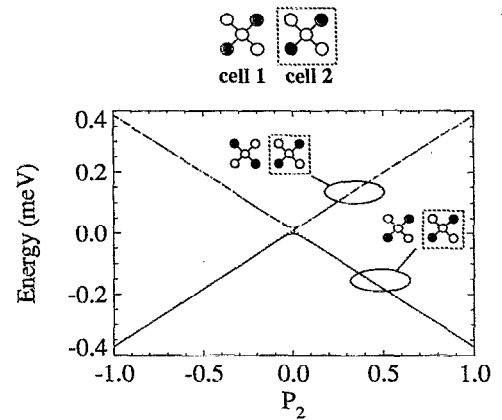


FIG. 2. The eigenstate energies for cell 1 as a function of the polarization of adjacent cell 2. The polarization of the eigenstates is indicated by the inset diagrams. The low-energy state is always the one with the same polarization as the “driver” cell 2. Slight exchange splitting (between the spatially symmetric and antisymmetric states) is evident for very small values of  $P_2$ .

To maintain charge neutrality, a fixed positive charge  $\tilde{\rho}$  with magnitude  $(2/5)e$  is assumed at each site. If cells had a net total charge then electrons in cells at the periphery of a line of cells would tend to respond mostly to the net charge of the other cells. In a semiconductor realization, the neutralizing positive charge would be provided by ionized donor impurities and charge on the surface of metal gates.

### C. Calculating the cell-cell response function

To be useful in cellular automata-type architectures,<sup>10</sup> the polarization of one cell must be strongly coupled to the polarization of neighboring cells. Consider the case of two nearby cells shown in the inset of Fig. 2. Suppose the charge distribution in the right-hand-side cell, labeled cell 2, is fixed. We assume cell 2 has polarization  $P_2$ , and that the charge density on site 0 is negligible (this means the charge density is completely determined by the polarization). For a given polarization of cell 2, we can compute the electrostatic potential at each site in cell 1. This additional potential energy is then included in the total cell Hamiltonian. Thus, the perturbing Hamiltonian is

$$H_{\text{inter}}^{\text{cell}} = H_1^{\text{cell}} = \sum_{i \in \text{cell } 1, \sigma} V_i^1 n_{i,\sigma}, \quad (5)$$

where

$$V_i^m = \sum_{k \neq m, j} V_Q \frac{(\rho_j^k - \tilde{\rho})}{|\mathbf{R}_{k,j} - \mathbf{R}_{m,i}|} \quad (6)$$

is the potential at site  $i$  in cell  $m$  due to the charges in all other cells. We denote the position of site  $j$  in cell  $k$  as  $\mathbf{R}_{k,j}$  and the single-particle density at site  $j$  in cell  $k$  as  $\rho_j^k$ . The total Hamiltonian for cell 1 is then

$$H^{\text{cell}} = H_0^{\text{cell}} + H_1^{\text{cell}}. \quad (7)$$

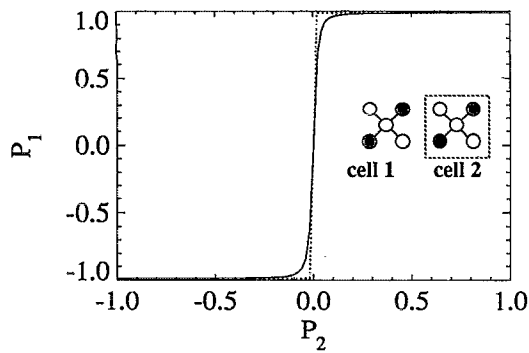


FIG. 3. The cell-cell response function (after Ref. 3). The induced cell polarization  $P_1$  is plotted as a function of the neighboring cell polarization  $P_2$ . The solid line shows the polarization of the spin-antisymmetric state and the dotted line shows the polarization of the (nearly degenerate) spin-symmetric state.

The two-electron Schrödinger equation is solved using this Hamiltonian for various values of  $P_2$ . The ground-state polarization of cell 1,  $P_1$ , is then computed as described in the previous section.

Figure 2 shows the splitting between the ground state and first excited state of cell 1 as a function of  $P_2$ . (Actually, each state is an exchange-split pair of spatially symmetric and antisymmetric states, but the splitting is hardly resolved at the energy scale shown here.) The perturbation rapidly separates states of opposite polarization. The excitation energy for a completely polarized cell to an excited state of opposite polarization is about 0.8 meV for our standard cell. Figure 3 shows  $P_1$  as a function of  $P_2$ —the cell-cell response function. A very small polarization in cell 2 causes cell 1 to be very strongly polarized. As the figure shows, the polarization saturates very quickly to either  $P = +1$  or  $P = -1$ . This bistable saturation is the basis of the effects described in this article.

As discussed at greater length in Ref. 4, the abruptness of the cell-cell response function depends on the ratio of the kinetic energy coupling parameter,  $t$  in Eq. (2), to the Coulomb terms in the Hamiltonian. The magnitude of  $t$  depends exponentially on both the distance between the dots and the height of the potential barrier between them.

### III. HARTREE SELF-CONSISTENT SOLUTION FOR MANY CELLS

In the analysis of the previous section, the two-electron eigenstates were calculated for a single cell. It is important to note that for the Hamiltonian employed these are exact two-particle eigenstates. This was possible because we could explicitly enumerate all possible two-electron states and diagonalize the Hamiltonian in this basis set. We now want to analyze linear arrays of many cells. Exact diagonalization methods then become intractable because the number of possible many-electron states increases rapidly as the number of electrons increases. We must therefore turn to an approximate technique.

The potential at each site of a given cell depends on the charge density at each site of all other cells. We will treat

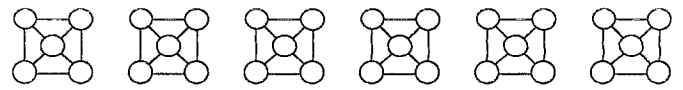


FIG. 4. A linear array of interacting cells. Each cell holds two electrons. Hopping between cells is assumed to be completely suppressed,

the charge in all other cells as the generator of a Hartree-type potential and solve iteratively for the self-consistent solution in all cells. This approximation, which we call the intercellular Hartree approximation (ICHA), can be stated formally as follows. Let  $\Psi_0^k$  be the two-electron ground-state wave function for cell  $k$ . We begin with an initial guess for the densities. Then, for each cell we calculate the potential due to charges in all other cells using Eq. (6). Although the neighboring cells will normally dominate, we do not restrict the analysis to near-neighbors only, but include the effect of all other cells. For a cell  $k$ , this results in a perturbation of the isolated cell Hamiltonian of Eq. (2):

$$H_k^{\text{cell}} = \sum_{i \in \text{cell } k, \sigma} V_i^k n_{i, \sigma}. \quad (8)$$

The Schrödinger equation for each cell is now solved for the two-electron ground-state eigenfunction,

$$(H_0^{\text{cell}} + H_k^{\text{cell}}) |\Psi_0^k\rangle = E_0^k |\Psi_0^k\rangle. \quad (9)$$

From the ground-state eigenfunctions we calculate the improved single-particle densities,

$$\rho_j^k = \sum_{\sigma} \langle \Psi_0^k | n_{j, \sigma} | \Psi_0^k \rangle. \quad (10)$$

The improved densities are then used in Eq. (6) and the system is iterated until convergence is achieved. Once the system converges, the many-electron energy  $E_{\text{tot}}$  is computed from the sum of the cell eigenenergies using the usual Hartree correction term to account for overcounting of the Coulomb interaction energy between cells,

$$E_{\text{tot}} = \sum_k E_k^0 - \sum_{k > q, i, j} V_Q \frac{\rho_i^k \rho_j^q}{|\mathbf{R}_{k,i} - \mathbf{R}_{q,j}|}. \quad (11)$$

It should be stressed that the ICHA still treats Coulombic, exchange, and correlation effects between electrons in the same cell exactly. The Hartree mean-field approach is used to treat self-consistently the interaction between electrons in different cells.<sup>11</sup>

It is relevant to point out that we do not require coherence of the many-electron wave function across the whole array of cells. All that is required to support this analysis is that the wave function is coherent across a single cell. No information about the phase of the wave function in other cells is relevant to the wavefunction in a given cell—only the charge densities in other cells need be known.

### IV. LINES OF QUANTUM CELLS

Figure 4 shows schematically a line of two-electron quantum cells. The distance between centers of adjacent

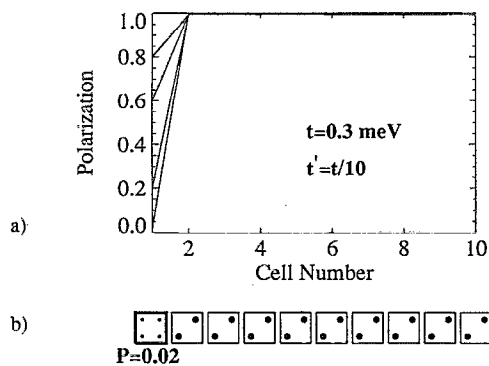


FIG. 5. The response of a line of cells. The polarization of cell 1 [shown in (b) with a darker outline] is fixed and the ground-state polarization induced in the line of cells is calculated. The plot shows the induced polarization for a driver polarization of  $P=0.9, 0.8, 0.6, 0.4, 0.2$ , and  $0.02$ . For the case of the weakest driver polarization,  $P=0.02$ , the charge densities on each site are shown in (b). The diameter of each dot is proportional to the charge density on that site. The Hamiltonian parameters used here are those of the "standard cell" discussed in the text. The result shows that even a slight polarization in a driver cell induces nearly complete polarization in the line of cells.

cells is three times the near-neighbor distance between dots in a single cell. If the polarization of the end cell is fixed, say to  $P=+1$ , a polarization will be induced in the neighboring cells. The question we address in this section is whether the saturation is sufficiently nonlinear that the entire line of cells will be "locked in" to a positive polarization. If this occurs for physically reasonable values of the Hamiltonian parameters, then lines of cells can perhaps be viewed as "wires" which transmit information, coded in the cell polarization, from one place to another.

### A. Line saturation

Figure 5 shows the polarization as a function of cell number for a line of 10 cells. The polarization of cell 1 is set to values of  $P=0.9, 0.8, 0.6, 0.2$ , and  $0.02$ , and the ground state of the electrons in the remaining nine cells is calculated self-consistently using the ICHA method described in the preceding section. The Hamiltonian parameters for these cells are those of the standard cell. These parameters yield a very bistable cell response. The result is that even a slight polarization in the driver cell results in essentially complete polarization of all other cells in the line, as is clear in the figure. Figure 5(b) is a plot of the calculated particle densities on each site in the line of cells for the case when the driver cell is polarized with only  $P=0.02$ . This figure is not a schematic representation, but a plot of the calculated single-particle densities. The radius of each dot shown is proportional to the particle density at the corresponding site. The squares around the cells are aids to the eye only; the driver cell is indicated with a darker square around it.

As the tunneling energies  $t$  and  $t'$  are increased, the two-particle ground-state wave function in each cell becomes less localized in the antipodal sites—the kinetic energy term begins to balance and eventually dominate the Coulomb term in the Hamiltonian. Figure 6 shows the

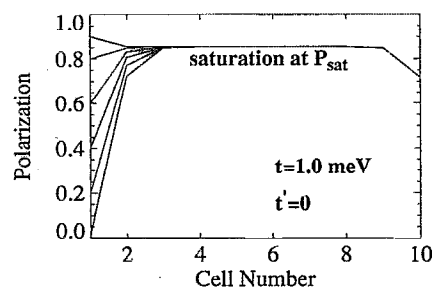


FIG. 6. The response of a line of cells for a different value of tunneling energy parameter. As in Fig. 5, the polarization of cell 1 is fixed and the ground-state polarization induced in the line of cells is calculated. The plot shows the induced polarization for a driver polarization of  $P=0.9, 0.8, 0.6, 0.4, 0.2$ , and  $0.02$ . The model cells here differ from the standard cells used for Fig. 5 in that the tunneling energy  $t$  is  $1.0$  meV and  $t'$  is neglected. The result shows that even a slight polarization in a driver cell induces a polarization in the line of cells but that the polarization saturates at a value  $P_{\text{sat}}$  (here about  $0.85$ ).

polarization of the line when  $t=1.0$  meV and  $t'=0$ . Figure 7 illustrates the case when  $t=1.0$  meV and  $t'=t/10$ . (The polarization of the last cell is always slightly lower because it has only one near neighbor.) Notice that in both cases the polarization saturates at a constant value, which we denote  $P_{\text{sat}}$ , several cells away from the driver cell. If the driver is polarized at a value larger than  $P_{\text{sat}}$ , the polarization decreases in successive cells until it reaches  $P_{\text{sat}}$ . If the driver is polarized at a value smaller than  $P_{\text{sat}}$ , the polarization increases in successive cells until it reaches  $P_{\text{sat}}$ . The value of  $P_{\text{sat}}$  depends on the physical parameters in the cell Hamiltonian and on the distance between cells.

If the driver cell has a fixed negative polarization, then the line will polarize to a saturation value of  $-P_{\text{sat}}$ . The undriven line has two degenerate ground states of opposite

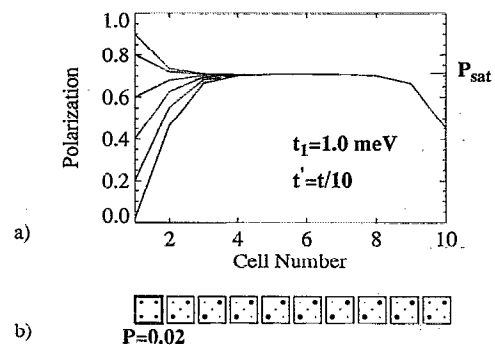


FIG. 7. The response of a line of cells for a different value of tunneling energy parameter. The polarization of cell 1 is fixed and the ground-state polarization induced in the line of cells is calculated. The plot shows the induced polarization for a driver polarization of  $P=0.9, 0.8, 0.6, 0.4, 0.2$ , and  $0.02$ . For the case of the weakest driver polarization  $P=0.02$ , the charge densities on each site are shown in (b). The diameter of each dot is proportional to the charge density on that site. The model cells here differ from the standard cells used for Fig. 5 in that the tunneling energy  $t$  is  $1.0$  meV and  $t'=t/10$ . The result shows that even a slight polarization in a driver cell induces a polarization in the line of cells but that the polarization saturates at a value  $P_{\text{sat}}$  (here about  $0.7$ ) which characterizes the response of the line.

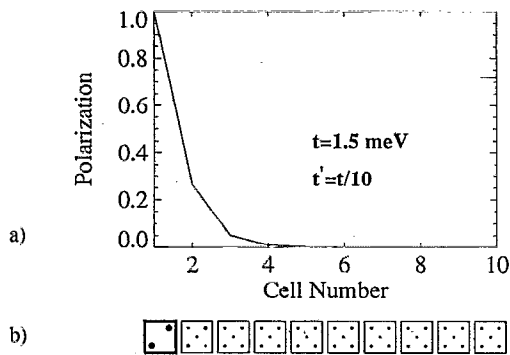


FIG. 8. Failure of a driver cell to polarize the line. In this case the tunneling parameters are chosen so that  $t=1.5$  meV and  $t'=t/10$ . The result is that the kinetic energy term in the Hamiltonian [Eq. (2)] overwhelms the Coulombic terms. A driver cell which is completely polarized then induces only a small polarization in its neighbors, and the polarization decays quickly down the line. The charge densities are shown in (b).

polarizations. The perturbation of the driver essentially selects one of these states as the new ground state, although it also modifies it in the region near the driver. Since we can change the signs of all polarizations, including the fixed drivers, and obtain another ground-state configuration (a mirror image of the original), we need here only consider situations with a positive polarization driver cell.

Figure 8 shows the cell polarization for a line of cells when the line “fails.” The kinetic energy parameters for this case are  $t=1.5$  meV and  $t'=t/10$ . Since the value of  $t$  is significantly larger than the Coulomb-induced splitting between the energy of oppositely polarized states (about 1 meV), the bistable response of the cells is very small. Thus, even a completely polarized driver cell fails to polarize the line. The polarization drops precipitously to zero.

Two important conclusions follow from these results. First, for a line of cells for which the tunneling energies  $t$  and  $t'$  are small enough to yield strong bistable behavior, a line of cells acts like a binary wire. That is, it robustly transmits a  $P=+1$  or  $-1$  polarization from one end to another. In fact it has the very attractive feature that it restores degraded signals back to the signal rails ( $P \cong \pm 1$ ). Second, the behavior of the line as a whole is characterized by the saturation polarization,  $P_{\text{sat}}$ . If  $P_{\text{sat}}$  is close to unity, the line functions very well as a binary wire. If the individual cells are not strongly bistable enough, the value of  $P_{\text{sat}}$  will be significantly less than unity and the line of cells will be less effective as a binary wire. If the bistability is sufficiently weak,  $P_{\text{sat}}$  is zero. In the following subsection we examine  $P_{\text{sat}}$  as a function of the physical parameters which specify the cell Hamiltonian.

## B. Dependence of $P_{\text{sat}}$ on physical parameters

For a long line of cells, all the cells sufficiently removed from the ends will have polarization  $P_{\text{sat}}$ . The infinite line contains two degenerate ground states with  $P = \pm P_{\text{sat}}$ . We calculate  $P_{\text{sat}}$  by considering a segment of an infinite line. Figure 9 shows a “target” cell with three neighbors on each side (more distant neighbors have a negligible influence on

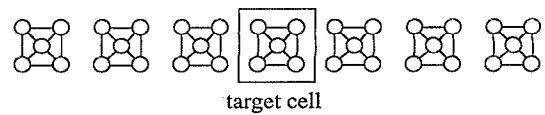


FIG. 9. Schematic view of cell geometry used in self-consistent calculation of the polarization of an infinitely long chain of cells.

the target cell). In the ground state all these cells have the same polarization  $P_{\text{sat}}$ . We solve for  $P_{\text{sat}}$  iteratively using the following scheme: All six neighbors are set to a polarization corresponding to an initial guess. The resulting potentials on the sites of the target cell are calculated and the two-electron Schrödinger equation is solved for the ground state of the target cell. The (induced) polarization of the target cell is then calculated from the two-electron wave function. The polarization of the six neighbors is now set to this calculated value and the process is iterated. The iteration converges to a fixed point when all cells have the same polarization  $P_{\text{sat}}$ . The saturation polarization calculated this way is identical to that obtained by considering a long (e.g., 20 cell) line and finding the polarization of the innermost cells.

We focus on the dependence of the saturation polarization as a function of the physical parameters which enter the cell Hamiltonian [Eq. (2)]. Figure 10 shows the variation of  $P_{\text{sat}}$  with the kinetic energy parameter  $t$  with  $t'=t/10$ . All other parameters are kept fixed. This is equivalent to changing the barrier height between the quantum dots. Higher values of  $t$  correspond to lower barrier heights. As the figure illustrates, for values of  $t$  above about 1 meV (a barrier height of roughly 100 meV for the standard cell), the saturation polarization falls quickly to zero. The transition occurs near  $t=1$  meV because that is roughly the energy splitting between the ground state and the excited state of opposite polarization (see Fig. 2). When the kinetic energy gain in hopping to neighboring sites balances this cost, the tendency of the cell to polarize is lost.

Figure 11 illustrates the variation of  $P_{\text{sat}}$  with  $a$ , the near-neighbor distance between quantum dots. As  $a$  is varied,  $t$  and  $t'$  are kept constant. The intercellular distance is

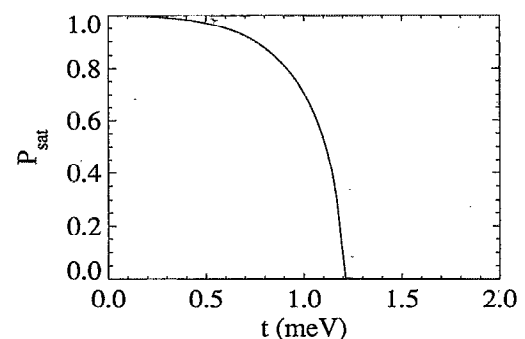


FIG. 10. The saturation polarization for an infinite linear chain of cells as a function of the tunneling parameter  $t$ . Other cell Hamiltonian parameters are fixed at the “standard cell” values.

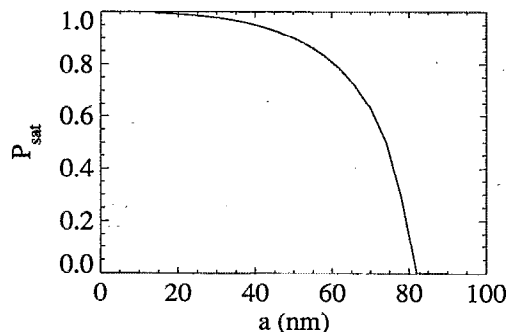


FIG. 11. The saturation polarization for an infinite linear chain of cells as a function of the near-neighbor site distance  $a$  (see Fig. 1). Other cell Hamiltonian parameters are fixed at the “standard cell” values.

always  $3a$ . The variation of  $a$  then has principally the effect of changing the strength of the Coulomb interaction between the cells and between dots in the same cell. The larger  $a$ , the weaker the Coulomb interaction and hence the weaker the bistable cell behavior.

Although we have focused on results for a particular “standard” cell with the specific physical parameters stated above, the saturation behavior is clearly determined by the ratio of the physical parameters, not their absolute values. Consider again the cell Hamiltonian in Eq. (2). The value of  $E_0$  will not affect the polarization behavior because it simply adds a constant shift to the total energy. We set  $t' = t/10$  for the near-neighbor and next-nearest-neighbor kinetic energy terms. The value of  $P_{\text{sat}}$  is then determined by three values: the kinetic energy parameter  $t$ , the site-site Coulomb energy parameter  $V_Q/a$ , and the on-site Coulomb term  $E_Q$ .

Let us examine what these three energy parameters correspond to physically. The energy  $t$  is half the value of the splitting between the spatially symmetric and antisymmetric states of a system of two quantum dots. It can also be considered as a hopping energy between neighboring dots which lowers the total energy by allowing the wave function to spread out spatially. The energy  $V_Q/a$  is the Coulomb energy of two electrons separated by the distance  $a$  (the near-neighbor interdot separation). The energy  $E_Q$  is the Coulomb energy of two electrons of opposite spin occupying the same quantum dot. It is roughly inversely proportional to the dot diameter.<sup>12</sup>

Consider the three-dimensional parameter space spanned by these three physical energies  $t$ ,  $V_Q/a$ , and  $E_Q$ . Systems with the same ratio of  $t:V_Q/a:E_Q$  have identical saturation behavior. The locus of equivalent systems is a ray passing through the origin in parameter space. Therefore, to explore saturation polarization for the entire parameter space spanned by these three physical parameters, it is sufficient to calculate  $P_{\text{sat}}$  on the surface of a sphere in the parameter space. This is shown in Fig. 12. The  $t$  axis has been scaled by a factor of 10. The values of  $P_{\text{sat}}$  are plotted through the gray-scale map shown. The map is nonuniform and is chosen to accentuate the very abrupt

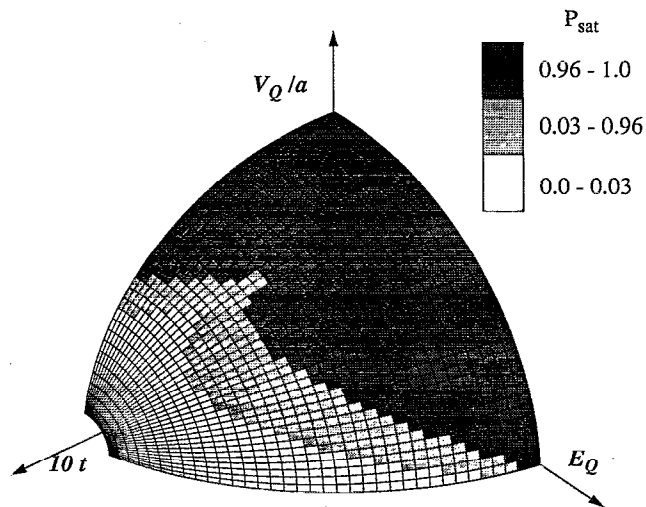


FIG. 12. The values of  $P_{\text{sat}}$  for the parameter space spanned by the parameters in the Hamiltonian.

transition between values of  $P_{\text{sat}}$  near unity and values very close to zero.

Figure 12 shows that the saturation behavior is not limited to an “island” in the Hamiltonian’s parameter space but is “continental.” Further, for most of the parameter space,  $P_{\text{sat}}$  is very close to 1 or 0. The transition is quite abrupt. A detailed examination of the interplay between on-site charging effects and near-neighbor effects awaits further study.

## V. DISCUSSION

The results presented suggest that the lines of quantum cells discussed here are indeed capable of forming binary wires in the following sense. Information is encoded in the polarization of individual cells. Say a bit value of 1 is represented by a polarization  $P = +1$  and a bit value of 0 is represented by a polarization of  $P = -1$ . Suppose the polarization of an end cell is fixed to 1 (perhaps electrostatically) and the line of cells is allowed to relax to its ground state. The ground state will be one for which all the cells have polarization 1 (bit value 1). If the end cell is switched, and the line again allowed to relax to its ground state, all the cells will switch to  $P = -1$  (bit value 0). This mechanism transports information, but not charge, from one end of the wire to another. It has the additional feature that inputs with polarization less than one, but still positive, will be “reset” to be 1. Similarly, degraded negative input polarizations will be reset to  $-1$ . The strong nonlinear bistable response of the coupled-cell system performs a role similar to gain in conventional digital devices, constantly restoring signal levels.

Note that in this scheme we rely on the ground-state configuration of the system—not the transient response. We assume inelastic processes are sufficient to relax the system to its new ground state after the input is changed. The wire “transmits” information in the sense that after

this relaxation has occurred, the new ground state is one in which the output end of the wire matches the input end.

In Ref. 4 we discuss the implementation of logical gates using the interacting quantum cells analyzed here. AND gates, OR gates, and inverters have all been designed using these ideas.

To function well, the cells need to be small enough that the Coulomb interaction between electrons in different dots is significant. Additionally, the effective barriers to tunneling between dots must be large enough that the kinetic energy advantage of spreading out the wave function does not overcome the Coulombic advantage of keeping the electrons in antipodal sites. As the results of Sec. IV B made clear, however, the relevant range of physical parameters is not a small, carefully balanced set.

Fabrication of such coupled dot structures surely represents a significant challenge, but the dimensions involved make it possible to conceive of semiconductor realizations using nanolithographic techniques presently being developed. Setting and reading the individual cell states at input and output ends involves the challenging task of sensing the presence of a single electron.

The theoretical analysis in this article is a zero-temperature treatment. At a nonzero temperature, entropy will become important. The excited states of a line have a much greater degeneracy (hence entropy) than the ground state. For long enough lines this means that the thermodynamic expectation value of the polarization will decay as the distance from the end driver cell increases. These effects will ultimately limit the size of usable binary wires and the operating temperatures feasible. Nevertheless, if the size scale can be sufficiently reduced (our standard cell is relatively large), more practical operating temperatures could be obtained.

In conclusion we have examined the behavior of lines of interacting quantum-dot cells. The bistable saturation in the cell-cell interaction results in "binary wire" behavior in which information, encoded in the cell polarization, can be robustly transmitted from one end of a line to another.

## ACKNOWLEDGMENTS

We gratefully acknowledge stimulating conversations with Wolfgang Porod and Gary Bernstein of the Notre

Dame Nanoelectronics Group. We would also like to thank Karl Hess and Anthony Leggett for helpful comments. This work was supported in part by the Advanced Research Projects Agency, the Office of Naval Research, and the Air Force Office of Scientific Research. This material is based in part upon work supported under a National Science Foundation Graduate Fellowship.

<sup>1</sup>R. T. Bate, *Bull. Am. Phys. Soc.* **22**, 407 (1977); J. N. Randall, M. A. Reed, and G. A. Frazier, *J. Vac. Sci. Technol. B* **7**, 1398 (1989); D. K. Ferry, L. A. Akers, and E. W. Greeneich, *Ultra Large Scale Interconnected Microelectronics* (Prentice-Hall, Englewood Cliffs, NJ, 1988).

<sup>2</sup>A general proposal involving coupled resonant-tunneling diodes has been discussed by the Texas Instruments group; see J. N. Randall, A. C. Seabaugh, Y.-C. Kao, J. H. Luscombe, and B. L. Newell, *J. Vac. Sci. Technol. B* **9**, 2893 (1991).

<sup>3</sup>C. S. Lent, P. D. Tougaw, and W. Porod, *Appl. Phys. Lett.* **62**, 714 (1993).

<sup>4</sup>C. S. Lent, P. D. Tougaw, W. Porod, and G. H. Bernstein, *Nanotechnology* **4**, 49 (1993).

<sup>5</sup>R. Landauer, *Phys. Today* **42**, 119 (1989).

<sup>6</sup>The similar behavior of various other model cells is discussed in C. S. Lent, P. D. Tougaw, and W. Porod, *J. Appl. Phys.* **74**, 3558 (1993).

<sup>7</sup>The ability to control quantum dot occupancies over as many as  $10^8$  dots using a back-gating technique has recently been reported by B. Meurer, D. Heitmann, and K. Ploog, *Phys. Rev. Lett.* **68**, 1371 (1992).

<sup>8</sup>A proposal for cells with single-electron occupancy has been made, but lacks the requisite bistable character; see P. Bakshi, D. A. Broido, and K. Kempa, *J. Appl. Phys.* **70**, 5150 (1991).

<sup>9</sup>The polarization so defined is not to be confused with a dipole moment. For the situations we consider here, the ground state of the cell has no dipole moment, although it may have a quadrupole moment. The cell polarization simply measures the degree to which the electronic charge is aligned and the direction of that alignment.

<sup>10</sup>T. Toffoli and N. Margolus, *Cellular Automata Machines: A New Environment for Modeling* (MIT Press, Cambridge, MA, 1987).

<sup>11</sup>Since electrons in different cells are physically distinguishable (there being no wave-function overlap), the exchange coupling between them is zero. The Hartree and Hartree-Fock approximations are therefore equivalent in this case.

<sup>12</sup>For the standard cell, we take  $E_Q$  to be the Coulomb energy of two electrons separated by one-third the dot diameter  $D$ , a physically reasonable first approximation. Varying  $E_Q$  is roughly equivalent to changing  $D$ .